J. Fluid Mech. (1992), *vol.* 243, *pp.* 171–181
Printed in Great Britain

Stokes flow of a cylinder and half-space driven by capillarity

By ROBERT W. HOPPER
Chemistry and Materials Science Department, Lawrence Livermore National Laboratory, Livermore, CA 94550, USA

(Received 26 August 1991 and in revised form 10 March 1992)

The coalescence of a cylinder with half-space by creeping viscous flow driven solely by surface tension is analysed using methods developed previously. The evolution of the shape with time is described, exactly, in terms of a time-dependent mapping function $z = \Omega(\zeta, t)$ of the upper half-plane, conformal on $\operatorname{Im}\zeta \geqslant 0$. The results are in closed analytic form except for the time, which requires a quadrature. The height of the figure decays as t^{-1} as $t \rightarrow \infty$, which is consistent with Kuiken's analysis of an isolated disturbance. (Previously, the author reported an erroneous solution which behaved otherwise.) The results are compared with the coalescence of equal cylinders obtained previously. For a modest degree of coalescence, the shapes are rather alike. In the limit as $t \rightarrow 0$, the time dependence of the minimum widths (necks) are the same. At the times when the minimum widths disappear, the heights of the two shapes are equal.

Appended is a note providing a counter-example to earlier conjecture. A simply connected region undergoing this type of flow need not remain so.

1. Introduction

This article treats the coalescence of a circular cylinder with half-space, by creeping viscous incompressible plane flow driven by surface tension. The time evolution of the shape is determined exactly – in simple, closed, analytic form except for the value of the time, which requires a quadrature. Internal velocity and stress fields are not obtained, though this is in principle straightforward. The subject is relevant to viscous sintering (Hopper 1984; Jagota & Dawson 1988; Kuiken 1990) and fibre optics technology, and is an interesting fluid mechanics problem in its own right. It is fundamentally nonlinear due to the large changes in shape, and it is emphasized that no mathematical approximations are made. The analysis employs a general method developed previously (Hopper 1990, 1991), in which the shape evolution is described in terms of a time-dependent conformal mapping from a fixed reference domain. References on related work are given in Hopper (1990, 1991), and an analysis of the coalescence of equal cylinders may be found in Hopper (1990). An article providing more details, in the context of materials science applications, is planned for publication elsewhere (Hopper 1992).

Regrettably, I previously disseminated erroneous information about this flow. This was based upon an analysis of the coalescence of two cylinders of unequal diameters. That analysis contained a grievous blunder, fortunately detected by Dr S. Richardson of Edinburgh University (personal communication, 1991).† One

† Dr Richardson, after discovering the error in my analysis of the coalescence of unequal cylinders, correctly described that flow (Richardson 1992). A differential equation connecting two

incorrect conclusion of the erroneous analysis was that the height of the shape above the plane remained constant in time, which was both counter-intuitive and at odds with a general result of Kuiken (1990) that an isolated disturbance on half-space should ultimately decay as t^{-1}. As will be seen, the shape does indeed decay in the manner given by Kuiken. I apologize to those I misled.

The general theory for a finite region regards it as the cross-section of an infinitely long isothermal general cylinder of Newtonian viscous liquid having dynamic viscosity η, density ρ and surface tension γ, in a gravitational field $\boldsymbol{g}$, all these being constant. The present case may, presumably, be imagined as the coalescence of a cylinder with some large region (such as a second cylinder or a square prism) that is allowed to become infinite in extent, and flat (in the infinite limit) on the side touching the circular cylinder. Let the initial diameter of the cylinder be D_0. A normalization scheme, detailed in Hopper (1990), is carried out using D_0 as the characteristic length. Denoting the position vector $\boldsymbol{x}_0$ and the time t_0, the corresponding dimensionless variables are $\boldsymbol{x} = \boldsymbol{x}_0/D_0$ and $t = \gamma t_0/\eta D_0$. Formally, the Navier–Stokes momentum equation in dimensionless form then involves a Suratman number $\rho\gamma D_0/\eta^2$ and a Bond number $\rho g D_0^2/\gamma$. In the limit where these approach zero, the equations of motion in dimensionless form reduce to those of Stokes: $\nabla^2 \boldsymbol{u} = \nabla p$, $\nabla \cdot \boldsymbol{u} = 0$. In practice, the Suratman number can often be made small independent of size by raising the viscosity η (for example, by a temperature change); a small Bond number requires a small size or microgravity environment. The boundary condition is that the surface traction is normal to the boundary and of magnitude equal to its curvature. An additive constant pressure would have no effect.

As discussed in Hopper (1990), the applicability of the analysis is subject to certain limitations. The surface tension of a real liquid depends on the local curvature if it is large enough, and on the separation of two surfaces if they are close enough. Primarily for this reason, the situation near the neck surface may in the very earliest stages of coalescence fail to satisfy the model. For finite regions, plane flow is an assumption that is applicable in variable degree. If the ends of the general cylinder are free, then capillarity induces a general axial flow, causing the body to shorten and its cross-sectional area to increase. In the present case, where a portion of the region has become infinite, the surface tension forces causing the axial flows are negligible compared with those of the circular cylinder of finite diameter, and the flow is strictly planar. Inertial effects are totally neglected, and no analysis of the magnitude of the inertial terms (of the Navier–Stokes momentum equation) will be attempted for the fields implicit in the present analysis. While it is not possible *a priori* to assure that inertial effects are negligible for all times, nothing about the behaviour suggests otherwise.

Leaving aside these issues, we now take Stokes' equations (momentum and continuity) for plane flow together with the classical surface traction boundary condition, in dimensionless forms, as the starting point. Let $z = \Omega(\zeta, t)$ conformally map $\mathrm{Im}\,\zeta \geqslant 0$ onto the (dimensionless) region representing the cylinder coalescing with half-space. Primes denote complex derivatives with respect to the independent (complex) variable; an overdot, the derivative with respect to time; and an asterisk, the complex conjugate. Let $\xi = \mathrm{Re}\,\zeta$. The surface tractions are intrinsic in the map $\Omega(\zeta, t)$. By considering the requirements that the surface velocity be such that a point $z = \Omega(\xi, t)$ move to $z + \mathrm{d}z = \Omega(\xi + \mathrm{d}\xi, t + \mathrm{d}t)$ in the time increment $\mathrm{d}t$, and that the

of the four map parameters must be solved numerically, with a subsequent quadrature still required for the time.

boundary condition for the surface traction equation be satisfied, the following expression (equation (30a), Hopper 1991) giving the values of a certain function $\psi(\xi, t)$ in terms of $\Omega(\xi, t)$ was obtained:

$$\mathrm{i}\psi(\xi,t) = \Omega(\xi,t)^*\left[\frac{\Omega''(\xi,t)}{\Omega'(\xi,t)}G(\xi,t)+G'(\xi,t)-\mathrm{i}\frac{\dot{\Omega}'(\xi,t)}{\Omega'(\xi,t)}\right]+\Omega'(\xi,t)^*G(\xi,t)-\mathrm{i}\dot{\Omega}(\xi,t)^*. \quad (1)$$

$G(\zeta)$ is defined by the Cauchy integral

$$G(\zeta,t) = \frac{1}{2\pi\mathrm{i}}\int_{-\infty}^{\infty}\frac{1}{|\Omega'(\xi,t)|}\frac{1}{\xi-\zeta}\mathrm{d}\xi, \quad \mathrm{Im}\,\zeta > 0. \quad (2)$$

With the boundary values given by a Sokhotskyi (Plemelj) formula, (2) defines a single function analytic on $\mathrm{Im}\,\zeta \geqslant 0$. In practice, a suitable parametric form $\Omega[\zeta; a_1(t), a_2(t), \ldots]$ must be conjectured – i.e. guessed. The basic condition of the theory is that $\psi(\xi, t)$ be the boundary value of a function analytic throughout $\mathrm{Im}\,\zeta \geqslant 0$ for $t > 0$; that is, that the function on the real line can be continued analytically onto the upper half-plane. The chosen form is validated by demonstrating that this is possible, and the time dependences of the parameters are determined by actually doing so.

2. Analysis

The following mapping function is conjectured:

$$\Omega(\zeta,t) = -\left[\zeta+\frac{a(t)\,h(t)}{\zeta+\mathrm{i}a(t)}\right], \quad \mathrm{Im}\,\zeta \geqslant 0, \quad t > 0, \quad (3)$$

where $a(t) \to 0$ and $h(t) \to 1$ as $t \to 0$, and $a(t) \to \infty$ as $t \to \infty$. Informally, the pole at $\zeta = -\mathrm{i}a$ draws the line $\mathrm{Im}\,\zeta = 0$ into a circle as $t \to 0$; allowing the strength of the pole to decrease as $a \to 0$ enables the circle to be kept finite and localized as $t \to 0$; and moving the pole to infinity leaves a straight line as $t \to \infty$. It will be seen presently that this map indeed has adequate flexibility to describe the time-evolution of the flow of a region that, as $a \to 0$, consists of the lower half-plane together with a disk of unit diameter centred at $z = \frac{1}{2}\mathrm{i}$. Obviously, $\Omega(0, t) = \mathrm{i}h(t)$ and $\Omega[\zeta \to (\pm\infty + \mathrm{i}0), t] = (\mp\infty - \mathrm{i}0)$.

The analysis is much like that of the isolated groove treated previously (Hopper 1991, §4). Upon using (3) in (1), it is found that the analytic continuation of $\psi(\xi)$ onto $\mathrm{Im}\,\zeta > 0$ involves terms causing, potentially, a pole of first and of second order at $\zeta = \mathrm{i}a$. These may be avoided by adjusting $a(t)$ and $h(t)$ so that the coefficients of $(\zeta - \mathrm{i}a)^{-1}$ and of $(\zeta - \mathrm{i}a)^{-2}$ vanish as $\zeta \to \mathrm{i}a$. The latter gives the condition

$$\dot{a} = G(\mathrm{i}a) \quad (4)$$

and the former leads (using (4)) to an expression that is easily rearranged and expressed as

$$4\mathrm{d}(ah)/\mathrm{d}t + \mathrm{d}(h^2)/\mathrm{d}t = 0. \quad (5)$$

Integrating and imposing the condition ($t \to 0$) that $h = 1$ when $a = 0$,

$$a = (1-h^2)/4h. \quad (6)$$

With (6) it is easily shown by direct integration that the area above $\operatorname{Im} z = 0$ is constant at $\frac{1}{4}\pi$. It is also straightforward to show that as $a \to 0$ the boundary becomes circular for $|\xi| \ll a$ and becomes a straight line for $|\xi| \gg a$.

Equation (4) becomes

$$\dot{a} = \frac{1}{2\pi \mathrm{i}} \int_{-\infty}^{\infty} (\xi + \mathrm{i}a)\{[\xi^2 - a(a+h)]^2 + 4a^2\xi^2\}^{-\frac{1}{2}} \mathrm{d}\xi. \tag{7}$$

Exploiting symmetry and using equation (3.165.2) of Gradshteyn & Rhyzhik (1980),

$$\dot{a} = \frac{1}{\pi}\left(\frac{a}{a+h}\right)^{\frac{1}{2}} \mathrm{K}\left[\left(\frac{h}{a+h}\right)^{\frac{1}{2}}\right]. \tag{8}$$

Here $\mathrm{K}(k)$ is the complete elliptic integral of the first kind defined by

$$\mathrm{K}(k) = \int_0^{\pi/2} (1 - k^2 \sin^2\varphi)^{-\frac{1}{2}} \mathrm{d}\varphi. \tag{9}$$

Define a new parameter

$$\mu = [h/(a+h)]^{\frac{1}{2}}. \tag{10}$$

The parameters are now interrelated by (6) $[a(h)]$ and by

$$h(\mu) = \frac{\mu}{(4-3\mu^2)^{\frac{1}{2}}}, \quad \mu(h) = \frac{2h}{(1+3h^2)^{\frac{1}{2}}} \tag{11a, b}$$

$$a(\mu) = \frac{1-\mu^2}{\mu(4-3\mu^2)^{\frac{1}{2}}}. \tag{12}$$

The stage of the coalescence is usually most conveniently specified with the parameter h. Equations (8) and (12) now give $\mathrm{d}\mu/\mathrm{d}t$, and the result may be integrated to give

$$t(\mu) = 2\pi \int_{\mu}^{1} \frac{2-k^2}{k^2(4-3k^2)^{\frac{3}{2}}(1-k^2)^{\frac{1}{2}}\mathrm{K}(k)} \mathrm{d}k. \tag{13a}$$

$t(\mu)$ must be integrated numerically, and it is helpful to eliminate the $(1-k^2)^{-\frac{1}{2}}$ factor with the substitution $k = \cos\vartheta$:

$$t(\mu) = 2\pi \int_0^{\cos^{-1}\mu} \frac{2-\cos^2\vartheta}{(\cos^2\vartheta)(4-3\cos^2\vartheta)^{\frac{3}{2}}\mathrm{K}(\cos\vartheta)} \mathrm{d}\vartheta. \tag{13b}$$

Equations (3), (11), (12) and (13) provide the complete solution of the problem for $t > 0$ in terms of the parameter μ. (The theory is both mathematically and physically invalid for the singular condition of $\mu = 0$; mathematically, μ may be taken arbitrarily close to zero.) A convenient parametric form for the Cartesian coordinates is

$$X(\xi) = \xi\left(1 + \frac{ah}{\xi^2 + a^2}\right), \quad Y(\xi) = \frac{a^2 h}{\xi^2 + a^2}. \tag{14a, b}$$

(Here and in the following the sign of ξ has been reversed, so that $\xi > 0$ gives $X > 0$.) One may also use the ordinate as the independent variable:

$$X(y) = \pm(y+a)(h/y - 1)^{\frac{1}{2}}. \tag{14c}$$

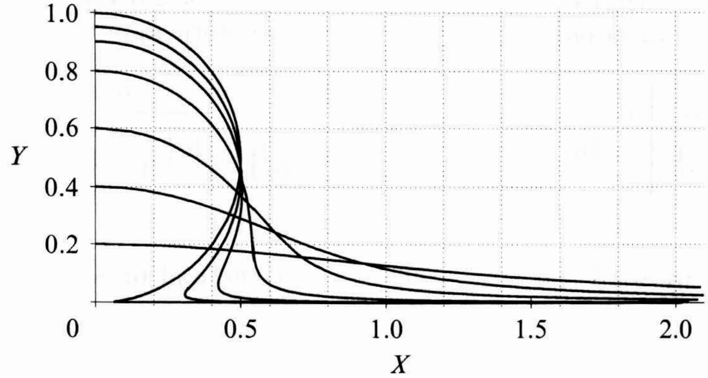

FIGURE 1. Coalescence of a cylinder into half-space. The shapes are those for $t = 0.035$, 0.248, 0.390, 0.631, 1.107, 1.749 and 3.207.

Typical shapes are shown in figure 1.

A few geometric features may be noted. As already mentioned, the height of the figure is just h. The minimum and maximum widths X_{min} and X_{max} occur at

$$\xi_{\text{min/max}} = \left\{\frac{1-h^2}{8h}\left[\frac{3h^2-1}{2h} \pm (3h^2-2)^{\frac{1}{2}}\right]\right\}^{\frac{1}{2}}, \tag{15a}$$

$$X_{\text{min/max}} = X(\xi_{\text{min/max}}) = \frac{3h\pm(3h^2-2)^{\frac{1}{2}}}{h\pm(3h^2-2)^{\frac{1}{2}}}\left\{\frac{1-h^2}{8h}\left[\frac{3h^2-1}{2h} \pm (3h^2-2)^{\frac{1}{2}}\right]\right\}^{\frac{1}{2}}, \tag{15b}$$

$$Y(\xi_{\text{min/max}}) = \frac{1-h^2}{2[h\pm(3h^2-2)^{\frac{1}{2}}]}. \tag{15c}$$

These disappear for $h < h_{\text{loss}} = (\frac{2}{3})^{\frac{1}{2}}$: the maximum and minimum widths merge with the inflexion when $h = h_{\text{loss}}$. At this point $\xi_{\text{loss}} = \frac{1}{8}\sqrt{2}$, $X_{\text{loss}} = \frac{3}{8}\sqrt{2} \approx 0.5303$, $Y_{\text{loss}} = \frac{1}{12}\sqrt{6} \approx 0.2041$, $\mu_{\text{loss}} = \frac{1}{3}\sqrt{8}$ and $t_{\text{loss}} \approx 0.5930$. Generally, the inflexion occurs at

$$\xi_{\text{infl}} = \frac{1}{4\sqrt{3h}}(1-h^2)^{\frac{1}{2}}(1+3h^2)^{\frac{1}{2}}, \tag{16a}$$

$$X(\xi_{\text{infl}}) = \frac{1}{4\sqrt{3h}}(1-h^2)^{\frac{1}{2}}(1+3h^2)^{\frac{3}{2}}, \tag{16b}$$

$$Y(\xi_{\text{infl}}) = \tfrac{3}{4}h(1-h^2). \tag{16c}$$

As $t \to \infty$ ($\mu \to 0$), the shape becomes

$$Y(\xi) \sim h[1+16h^2X(\xi)^2]^{-1}. \tag{17}$$

The following approximations to $t(\mu)$ may be obtained by approximating the integrand of (13a) with appropriate series' (Gradshteyn & Rhyzhik 1980, Sec. 8.113). For $t \to \infty$, integration provides a convergent series, the first few terms of which are

$$t(\mu) \approx t(\mu_0) + (1/\mu - 1/\mu_0) + \tfrac{7}{8}(\mu_0 - \mu) + \tfrac{25}{128}(\mu_0^3 - \mu^3) \quad \text{as} \quad \mu \to 0. \tag{18}$$

For $\mu_0 = 0.3$, $t(\mu_0) \approx 3.97147$. The error is then $< 0.1\,\%$ for $h < 0.4$ ($\mu < \sim 0.658$). For $t \rightarrow 0$, successive integrations by parts gives the asymptotic approximation

$$t(\mu) \sim \frac{2\pi(1-\mu^2)^{\frac{1}{2}}}{\ln\left(\frac{4}{(1-\mu^2)^{\frac{1}{2}}}\right)}\left[1-\frac{1}{\ln\left(\frac{4}{(1-\mu^2)^{\frac{1}{2}}}\right)}+\frac{2}{\left[\ln\left(\frac{4}{(1-\mu^2)^{\frac{1}{2}}}\right)\right]^2}-\frac{6}{\left[\ln\left(\frac{4}{(1-\mu^2)^{\frac{1}{2}}}\right)\right]^3}\right] \quad \text{as} \quad \mu \rightarrow 1. \tag{19}$$

This is accurate to $\sim 1\,\%$ for $h > 0.9999$ ($t < \sim 0.006$) and to $\sim 5\%$ for $h > 0.99$ ($t < \sim 0.09$).

3. Discussion

The coalescence of a cylinder with half-space in Stokes flow driven by surface tension has been described. The extent to which coalescence has progressed is conveniently specified by the parameter h, which is the height of the shape. The singular initial state is avoided by requiring $h < 1$. Equations (11)–(14) then provide a complete description for $t > 0$.

Kuiken (1990) analysed the damping of small disturbances on half-space undergoing plane viscous flow driven by capillarity. He found that the amplitude of a disturbance that initially is localized ultimately decays as t^{-1}. A disturbance that is initially extended, such as a wave, decays exponentially. The reason an extended disturbance decays more rapidly than a localized one is that the latter spreads out with time, so the curvature driving the flow decreases faster. For the same reason, exponential decay must eventually occur in the coalescence of two cylinders of arbitrary initial diameters. (If the ratio of initial diameters is large, one intuitively expects the exponential decay to set in only at quite large times – when the finiteness of the boundary finally prevents further spreading of the remnant of the smaller cylinder.) The expected t^{-1} behaviour is found here: at very long times, $h \sim 1/2t$. In this limit, the shape becomes

$$Y \sim \frac{1}{2t[1+(2X/t)^2]}. \tag{20}$$

Kuiken (1990) analysed directly the decay of the shape (20), in a small-amplitude limit. Under a suitable renormalization, the results are equivalent, demonstrated as follows. Let t^* be some large dimensionless time in the present analysis, such that (20), is an accurate approximation. Then renormalize using $D_0\,Y(0,t^*)$ as the characteristic length, and with the new time zero corresponding to t^*. In making the comparison, it is necessary to retain the 'ϵ' multiplier in Kuiken's (1990) (28)–(29). The equivalence then follows directly.

No purely analytic solution of the coalescence of cylinders of arbitrary diameter is available at this time. Presumably, however, most features of such flow will be bracketed by the two cases that are known – the cylinder and half-space, and the two equal cylinders. A comparison is therefore of interest. Equations for equal cylinders (Hopper 1990) are given in Appendix A. Variables subscripted '1' refer to the two-cylinder case. Figure 2(*a*) compares the shapes at the same time, while figure 2(*b*) shows the shapes at equal values of the minimum widths (see (A 4)). It is seen that for a modest degree of coalescence, the lobes in the two cases are rather similar. This merely reflects the fact that the forces driving the flows are comparable. In the

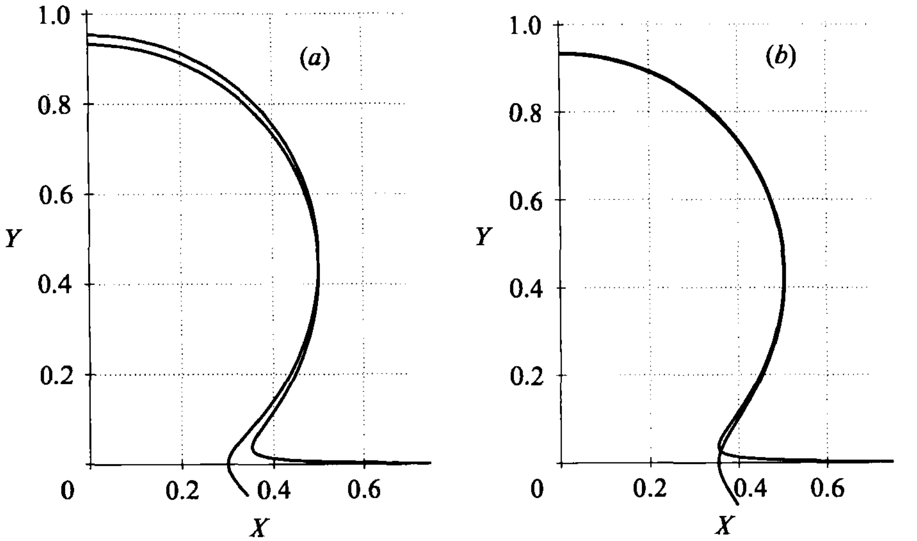

FIGURE 2. (*a*) Comparison of the coalescence of a cylinder and half-space with that of equal cylinders at $t = 0.300$. For the cylinder and half-space $X_{min} = 0.353$; for the equal cylinders, $X_{1min} = 0.300$. (*b*) Comparison of the coalescence of a cylinder and half-space with that of equal cylinders, when X_{min} is the same. For the cylinder and half-space $t = 0.300$; for the equal cylinders, $t_1 = 0.386$.

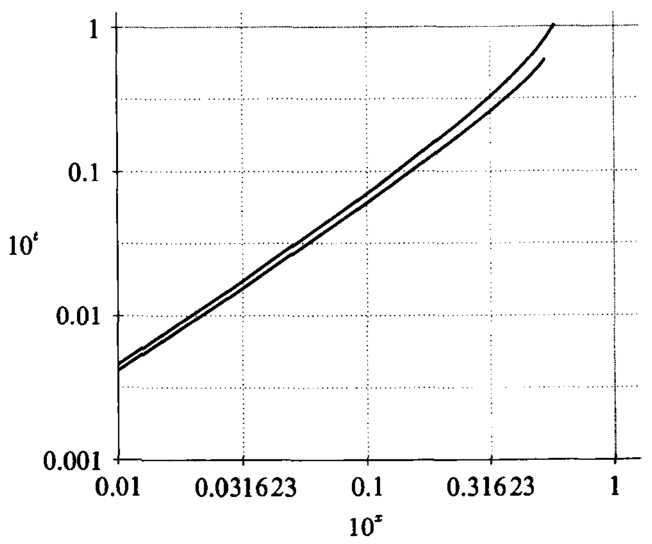

FIGURE 3. Minimum widths in the coalescence of a cylinder and half-space (lower curve), and in that of equal cylinders (upper curve) as a function of time. The log-log scale obscures the diverging likenesses of the shapes at long times.

coalescence of a pair of unequal cylinders it may therefore be expected that the shape of the smaller lobe, at a given dimensionless time, will depend only weakly upon the initial diameter ratio — again for a modest degree of coalescence and with the normalization done using the diameter of the *smaller* cylinder as the characteristic length. As a semi-quantitative guide, figure 3 shows $X_{min}(t)$ for the two cases, and figure 4 shows the shapes when their minimum widths are lost. It is remarkable that

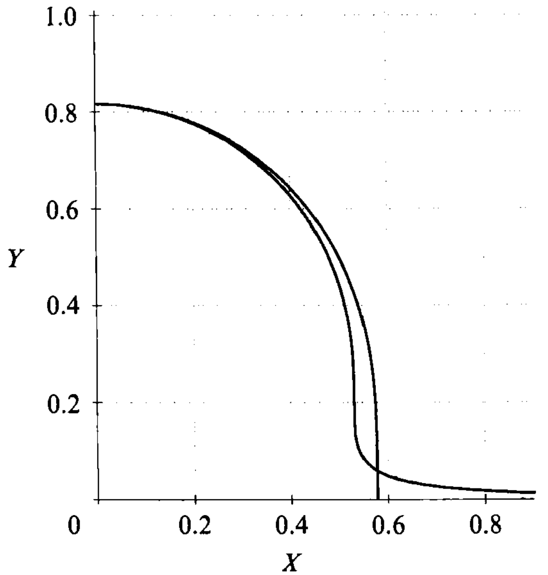

FIGURE 4. Comparison of the coalescence of a cylinder and half-space with that of equal cylinders, at the times when the minimum widths are lost ($t_{loss} \approx 0.5930$, $X_{min} \approx 0.5303$, $t_{1loss} \approx 1.02665$, $X_{1min} \approx 0.5774$). The heights of the two shapes are identical: $h = (\frac{2}{3})^{\frac{1}{2}}$.

the heights of the two shapes are then the same: $(\frac{2}{3})^{\frac{1}{2}} \approx 0.8165$. The obvious speculation is that this might be true of some characteristic vertical dimension for arbitrary initial diameters.

The very early time regime involves two slightly rounded cusps that nearly meet, a situation which may be of theoretical interest. Using the small-time approximations, (19) and (A 6), it is found that the time-dependances of X_{min} in the limit as $t \rightarrow 0$ are identical for both a cylinder on half-space and for equal cylinders:

$$t \sim \frac{\pi X_{min}}{\ln(4/X_{min})}. \tag{21}$$

Only the lead terms of these asymptotic approximations match. It is reasonable to presume that (21) holds for two cylinders of arbitrary diameter.

The theory of coalescence of equal cylinders (Appendix A) is in agreement with experimental observations of glass fibres near the softening point (Korwin, Eaton & Pye 1991). D. Korwin, S. Lange & L. Pye (personal communication, 1990) have studied experimentally at the New York State College of Ceramics at Alfred University, the coalescence of a fibre with a plate but have not yet compared the results with the present theory. (The plate thickness was about four fibre diameters.)

The author thanks Professor S. Richardson (University of Edinburgh) for thoughtful comments and, especially, for discovering the error in the analysis of unequal cylinders. Insightful comments by an anonymous referee of the (erroneous) unequal-cylinders manuscript were most helpful in clarifying inertial issues. This work was performed under the auspices of the US Department of Energy by the Lawrence Livermore National Laboratory under contract W-7405-ENG-48.

Appendix A. Formulae for the coalescence of equal cylinders

The coalescence of two equal cylinders was solved in Hopper (1990, §4.4). (Plane flow in this case is an *approximation*, the validity of which discussed in that reference. See also Hopper 1984.) In this Appendix, some analogous equations for the cylinder and half-space problem are presented. Notations correspond but are subscripted '1'. To facilitate comparison with the cylinder on half-space, the normalization of the equal-cylinder case is now based on the initial diameter, rather than the final radius, as the characteristic length.

The degree of coalescence is specified by a parameter ν, which decreases from 1 to 0 over time. One quadrant of the shape is given by

$$X_1(\xi) = \frac{1-\nu^2}{[2(1+\nu^2)]^{\frac{1}{2}}} \frac{1+\nu}{(1+\nu)^2-4\nu\xi^2}(1-\xi^2)^{\frac{1}{2}}, \tag{A 1a}$$

$$Y_1(\xi) = \frac{1-\nu^2}{[2(1+\nu^2)]^{\frac{1}{2}}} \frac{1-\nu}{(1+\nu)^2-4\nu\xi^2}\xi, \tag{A 1b}$$

with reflections completing it. The parameter ξ varies from 0 to 1. The curves (X_1, Y_1) all pass through the point $(\frac{1}{2}, \frac{1}{2})$. The time is

$$t_1(\nu) = \frac{\pi}{2\sqrt{2}} \int_\nu^1 [k(1+k^2)^{\frac{1}{2}} \mathrm{K}(k)]^{-1} \,\mathrm{d}k. \tag{A 2}$$

These results are equivalent to those in Hopper 1990 (equations (63) and (64)), and in Hopper 1984 (equation (5)) when allowance is made for the different normalizations.

The height and the minimum width are

$$Y_1(1) = (1+\nu)[2(1+\nu^2)]^{-\frac{1}{2}} \tag{A 3a}$$

and

$$X_{1\min} = X_1(0) = (1-\nu)[2(1+\nu^2)]^{-\frac{1}{2}}, \tag{A 3b}$$

respectively. $X_{1\min}$, $X_{1\max}$ and $X_{1\mathrm{infl}}$ merge and are lost at $\nu_{\mathrm{loss}} = 3-2(\sqrt{2}) \approx 0.1716$, at which point $X_1(0) = 1/\sqrt{3} \approx 0.5774$, $Y_1(1) = (\frac{2}{3})^{\frac{1}{2}} \approx 0.8165$ and $t_{1\mathrm{loss}} \approx 1.02665$. For a given $X_1(0)$, (A 3*b*) provides the corresponding value of ν:

$$\nu = \{1-2X_1(0)[1-X_1(0)^2]^{\frac{1}{2}}\}[1-2X_1(0)^2]^{-1}. \tag{A 4}$$

This is useful when comparing the two flows as in figure 2(*b*).

Approximate expressions for the time are

$$t_1(\nu) \approx 1/\sqrt{2}[\ln(1/\nu) + 3\nu^2/16 - 0.3199] \quad \text{as} \quad \nu \to 0, \tag{A 5}$$

$$t_1(\nu) \sim \frac{\pi}{4} \frac{1-\nu^2}{\ln[16/(1-\nu^2)]}\left[1 - \frac{1}{\ln[16/(1-\nu^2)]} + \frac{2}{\{\ln[16/(1-\nu^2)]\}^2}\right] \quad \text{as} \quad \nu \to 1. \tag{A 6}$$

The error in the former is $< 0.1\%$ for $\nu < 0.1$, while in the later it is $< 1\%$ for $\nu > 0.998$.

Appendix B. Non-maintenance of domain simplicity

The issue was raised in Hopper (1990) of whether a simply connected region undergoing plane Stokes flow driven by surface tension remains simply connected. A simple counter-example shows that this is not so. The counter-example is not

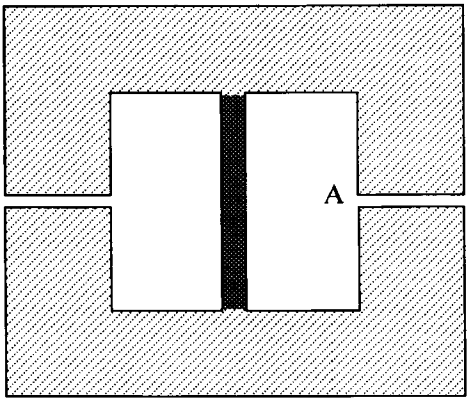

FIGURE 5. Simply connected region that will evolve to one that is not simply connected. See Appendix B.

analysed in detail, but the general nature of the flow is so evident that the conclusion can hardly be doubted. The region is depicted in figure 5. The following employs dimensional quantities. The body is centred on Cartesian coordinates (x_1, x_2), but these are not shown. The corners are drawn square but should be regarded as slightly rounded.

The net force, per unit depth of the body, applied to the cross-hatched central web by the surface-tension forces of the upper half of the body is $\boldsymbol{F} = -2\gamma \boldsymbol{i}_2$. If the width of the web is w, then the velocity field in the web will (except near the corners) be approximately $\boldsymbol{v} \approx (\gamma/2\mu w)(x_1 \boldsymbol{i}_1 - x_2 \boldsymbol{i}_2)$. The other parts of the body are subjected to net forces of comparable magnitude, but the resulting strain rates (except in the immediate vicinity of corners) will be much smaller owing to the large widths. Thus the thick regions will translate more or less rigidly with a velocity approximately that of the ends of the web. If the height of the web is h, then the velocity of the large sections of the upper half of the body will be $\sim (-\gamma h/2\mu w)$. In particular, this will be roughly the velocity of the line segment AB. Choosing w small, this motion is dominant, and some portion of AB will soon contact its lower counterpart. This would occur long before other large-scale changes of the boundary became significant. Deformation in the immediate vicinity of the corners, where the stresses are large, would not prevent contact. For sufficiently small w, with a constant γ/μ, inertia would be significant, but the question raised is purely one of Stokes flow, in which inertia is entirely omitted.

Thus, a simply connected region undergoing plane Stokes flow driven solely by surface tension need not remain simply connected. Note, however, that the counter-example is not a star domain.

REFERENCES

GRADSHTEYN, I. S. & RHYZHIK, I. M. 1980 *Table of Integrals, Series and Products*, (transl. A. Jeffrey, corrected and enlarged edn). Academic.

HOPPER, R. W. 1984 Coalescence of two equal cylinders – exact results for creeping viscous plane flow driven by capillarity. *J. Am. Ceram. Soc.* (*Commun.*) **67**, C262–264. See also errata *ibid.* **68**, C138 (1985).

HOPPER, R. W. 1990 Plane stokes flow driven by capillarity on a free surface. *J. Fluid Mech.* **213**, 349–375.†

† Most errors in Hopper (1990) are listed in Hopper (1991). In addition, the upper limit of the integral in (44) should be $\pi/2$. Hopper (1991) contains the following errors: In the first paragraph

HOPPER, R. W. 1991 Plane stokes flow driven by capillarity on a free surface. Part 2. Further developments. *J. Fluid Mech.* **230**, 355–364.†

HOPPER, R. W. 1992 Coalescence of two viscous cylinders by capillarity. *J. Am. Ceram. Soc.* (to be submitted).

JAGOTA, A. & DAWSON, P. R. 1988 Micromechanical modelling of powder compact – I. Unit problems for sintering and traction induced deformation. *Acta Metall.* **36**, 2551–2561.

KORWIN, D. M., LANGE, S. R., EATON, W. C., JOSEPH, I. & PYE, L. D. 1992 A study of the sintering behavior of glass in two geometric configurations. *Proc. 16th Intl. Congress on Glass.* In *Boletín de la Sociedad Española de Cerámica y Vidrio* (to appear).

KUIKEN, H. K. 1990 Viscous sintering: the surface-tension-driven flow of a liquid form under the influence of curvature gradients at its surface, *J. Fluid Mech.* **214**, 503–515.

RICHARDSON, S. 1992 Two-dimensional slow viscous flows with time-dependent free boundaries driven by surface tension. *Eur. J. App. Maths.* (to appear).

on p. 356, the name is Kolosoff (or Kolosov) not Kolostoff. In (3), the second term within braces should be $\sigma F''(\sigma)$, and the Ω in the final term should be overdotted. The equation in the second line of §2 should read ... $= \zeta^{-1}[1+\zeta^N/(N-1)]$. In (7), the a and b in the last term within braces should be overdotted, and the limit is as $\zeta \rightarrow 0$. The first a in (8) should be overdotted. The equality sign within the right-hand side of (15) should be a plus. There should be a closing parenthesis after the π in (16). There should be a closing bracket before the exponent of (18*b*). In (21), the second argument of Ω_N should be $\nu(t)$, and the closing parenthesis following ζ^{-1} should not be present. The expression in the next to the last line of p. 358 should be $(2/\pi)k^{-1+1/(N-2)}$. In the third line of the second paragraph of §3, '$z = dz = \ldots$' should read '$z + dz = \ldots$' In the line after (29), the parenthesis after t should be closing, and the exponent should be μ. The last numerical factor in (37) should be $[2(3)^{\frac{1}{2}}\pi]^{-1}$. Equation (38) should begin $t(\nu) = 2(3)^{\frac{1}{2}}\pi\int \ldots$. There should be a minus after the equality of (40*b*).